Visible and infrared spectroscopy of Pr^{3+} and Tm^{3+} ions in lead borate glasses

Visible and infrared spectroscopy of Pr³⁺ and Tm³⁺ ions in lead borate glasses

W A Pisarski[1,4]**, J Pisarska**[2]**, G Dominiak-Dzik**[3] **and W Ryba-Romanowski**[3]

[1] University of Silesia, Institute of Materials Science, Bankowa 12, 40-007, Katowice, Poland
[2] Silesian University of Technology, Department of Materials Science, 40-019 Katowice, Poland
[3] Institute of Low Temperature and Structure Research, Polish Academy of Sciences, 50-422 Wrocław, Poland

E-mail: wpisarsk@us.edu.pl

Abstract
The visible luminescence of Pr³⁺ and Tm³⁺ ions in lead borate glasses has been investigated as a function of activator concentration. The Judd–Ofelt analysis and the Inokuti–Hirayama model for energy transfer between activator ions have been applied for investigations of the radiative and non-radiative relaxation of the Pr and Tm excited states. Based on the luminescence decay curve analysis, the concentration quenching of the $^1D_2$ emission of Pr³⁺ and $^1G_4$ emission of Tm³⁺ ions has been attributed to cross-relaxation processes. The infrared spectroscopic measurements provide information on structural changes in the borate network initiated by optically active (Pr or Tm) ions. Contrary to the praseodymium ions, the thulium ions play an additional role as a glass-modifier in the $PbO–B_2O–Al_2O_3–WO_3$ composition.

1. Introduction

Among several optical materials belonging to the heavy metal oxide glass family, the PbO-based systems have a great significance for potential applications. In particular, lead germanate [1], lead titanate, lead tellurite [2] and lead bismuth gallate [3] glasses containing rare earth (Pr or Tm) ions have been extensively studied. Praseodymium [4] and thulium [5] ions in $PbO–Bi_2O_3–Ga_2O_3$ (PBG) glasses were investigated as potential hosts for 1.31 and 1.48 μm fibre-optic amplifiers, respectively. Also, the same class of PBG glassy system doped with rare earth ions appears to be promising for nonlinear optics [6].

Alkali borate glasses are a wide group of optical materials, which have received great attention in the literature. Recently, the optical properties of Pr³⁺ [7] and Tm³⁺ [8] ions in

---

[4] Author to whom any correspondence should be addressed.

alkali borate glasses were analysed. The addition of a heavy metal element (PbO) to the borate matrix significantly increases its optical nonlinearity [9]. Additionally, the $PbO–B_2O_3$ system with its extreme differences between the masses of the lead and the boron atom are of interest for spectroscopic investigations. Studies of $PbO–B_2O_3$ systems doped with Nd^{3+}, Sm^{3+}, Dy^{3+} [10], Ho^{3+} [11] and Er^{3+} [12, 13] ions have been reported while no information is available on the optical properties of Pr^{3+} and Tm^{3+} ions in multicomponent lead borate glasses, to our knowledge. The phonon energy of lead borate glass is considerably higher than fluoride glass. In consequence, these glasses doped with Pr and Tm ions are rather useless for NIR applications. However, this glass family may be interesting as a luminescent material emitting in the visible and UV spectral region.

This paper is focused on the visible and infrared spectroscopy of Pr^{3+} and Tm^{3+} ions in the $PbO–B_2O_3–Al_2O_3–WO_3$ system. A small amount of Al_2O_3 increases the glass stability whereas the addition of a small WO_3 admixture is promising for luminescence, as was demonstrated by optical measurements in Tm-doped $TeO_2–WO_3$ systems [14, 15]. The contribution of radiative and non-radiative processes to Pr and Tm excited state relaxation has been analysed using Judd–Ofelt theory and the Inokuti–Hirayama (I–H) model. The theoretical and experimental results were compared to the data obtained for alkali borate glasses and crystals as well as other PbO-based systems.

2. Experimental details

A series of lead borate glasses (in wt%): $(72.5 − x)PbO–18.5B_2O_3–5Al_2O_3–3WO_3–xLn_2O_3$ (Ln = Pr, Tm) was prepared by mixing and melting of appropriate amounts of lead oxide, boron oxide, aluminium oxide, tungsten oxide and rare earth oxide of high purity (99.99%, Aldrich Chemical Co.). The reagents were mixed homogeneously together in an agate ball mill for 2 h in the appropriate composition. In doped samples, the PbO was partially substituted by praseodymium or thulium ions in various concentrations ($x = 0.5–4.0$ wt%). Lead borate glasses containing rare earth ions (PBAW:Ln) were melted at 900 °C, quenched and annealed below T_g in order to eliminate the internal mechanical stresses.

Optical absorption spectra were recorded using a Varian 2300 UV–VIS–NIR spectrophotometer. The luminescence was excited with a Continuum Model Surelite I optical parametric oscillator pumped by a third harmonic of an Nd:YAG laser. The luminescence was dispersed by a 1 m double grating monochromator and detected with a photomultiplier with S-20 spectral response. Luminescence spectra were recorded using a Stanford SRS 250 boxcar integrator controlled by a computer. Luminescence decay curves were recorded and stored by a Tektronix TDS 3052 oscilloscope. All measurements were carried out at room temperature.

The IR transmission spectra in the frequency region 400–4000 cm^{-1} were taken on a BIORAD spectrometer using the KBr pellet disc technique.

3. Relations used for spectroscopic calculations

The radiative transition probabilities for excited levels of rare earth (Pr and Tm) ions were calculated using the standard Judd–Ofelt theory [16, 17]. The theoretical oscillator strength for each transition of Pr^{3+} and Tm^{3+} ions, within $4f^2$ and $4f^{12}$ configurations, was calculated. In performing the analysis, a constant value of 1.92 was used for n, the refractive index of the medium, which is in a good agreement with the value given by Pan *et al* [9]. The squared reduced matrix elements $\|U^t\|^2$ taken from Carnall *et al* [18] were used for the calculations. The Ω_t ($t = 2, 4, 6$) intensity parameters were found by a least squares fitting of the experimental
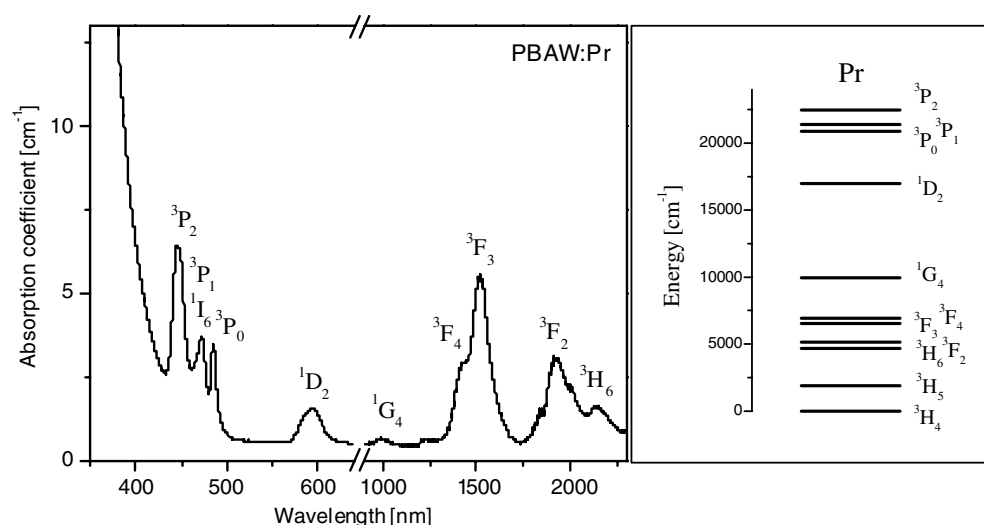
Figure 1. Absorption spectrum and energy level scheme of Pr-doped lead borate glass.

and theoretical electric dipole oscillator strengths. The Ω_t values were used to calculate the radiative transition probabilities, branching ratios and radiative lifetimes.

In order to estimate the ion–ion interaction, the Inokuti–Hirayama model [19] was applied for luminescence decay curve analysis. Considering a non-exponential character of the decay, the time evolution of the luminescence intensity was fitted to that predicted by the formula:

$$I(t) = A \exp[-(t/\tau_0) - \alpha(t/\tau_0)^{3/s}] \tag{1}$$

where A is a constant, $I(t)$ is the luminescence intensity after pulse excitation, τ_0 is the intrinsic lifetime of donor in the absence of acceptor, $s = 6$ for a dipole–dipole interaction between the ions, and α is the parameter given by the relation

$$\alpha = 4/3\pi\Gamma(1 - 3/s)N_a R_0^3 \tag{2}$$

where Γ is the Euler function, N_a is the concentration of acceptor ions and R_0 is the critical transfer distance defined as a donor–acceptor separation for which the rate of energy transfer between a donor–acceptor is equal to the rate of intrinsic decay rate τ_0^{-1}.

The Inokuti–Hirayama model is applicable only for analysis of energy transfer processes, where donor–acceptor transfer is faster than migration.

4. Results and discussion

4.1. Optical spectroscopy

4.1.1. Praseodymium. A room temperature absorption spectrum of Pr^{3+}-doped lead borate glass is presented in figure 1. The spectrum consists of two groups of inhomogeneously broadened absorption lines characteristic for 4f^2–4f^2 transitions of trivalent praseodymium, which are located in the visible and the infrared ranges, respectively. These lines correspond to the transitions from the $^3H_4$ ground state to the $^3H_6$, $^3F_2$, $^3F_3$, $^3F_4$, $^1G_4$, $^1D_2$, $^3P_0$, $^3P_1$, $^1I_6$ and $^3P_2$ excited states. The oscillator strengths of the observed transitions were obtained from the optical absorption bands. Next, the theoretical oscillator strengths were calculated basing on the Judd–Ofelt theory. Measured and calculated data are collected in table 1. The three Ω_t

Table 1. Measured and calculated oscillator strengths for Pr^{3+} ions in lead borate glasses. Transitions are from the $^3H_4$ ground state to the levels indicated. Wavelengths correspond to average transition energies. $\Omega_2 = 1.59$, $\Omega_4 = 3.40$, $\Omega_6 = 4.39$ (in 10^{-20} cm^2 units); rms $= 1.8 \times 10^{-6}$. The $^3P_2$ level was omitted from the Judd–Ofelt analysis.

Levels	Wavelength λ (nm)	Energy ν (cm^{-1})	Oscillator strengths		Residuals ($\times 10^{-6}$)
			$P_{meas.}$ ($\times 10^{-6}$)	$P_{calc.}$ ($\times 10^{-6}$)	
$^3H_6$, $^3F_2$	2000	5 000	3.860	3.861	0.001
$^3F_4$, $^3F_3$	1470	6 800	10.220	10.246	0.026
$^1G_4$	997	10 030	0.900	0.324	0.576
$^1D_2$	593	16 850	1.900	1.103	0.797
$^3P_0$	485	20 618	2.030	2.730	0.700
$^3P_1$, $^1I_6$	472	21 170	4.780	4.180	0.600

intensity parameters were evaluated from the least-squares fit of measured P_{meas} and calculated P_{calc} oscillator strengths. The phenomenological Judd–Ofelt parameters for Pr^{3+} ions in lead borate glasses are found to be $\Omega_2 = 1.59 \pm 0.75$, $\Omega_4 = 3.40 \pm 0.82$, $\Omega_6 = 4.39 \pm 0.31$ in 10^{-20} cm^2 units. The quality of the fit can be expressed by the magnitude of the root-mean-square (rms) deviation, defined by $\Sigma\,(P_{meas} - P_{calc})^2$. The rms deviation of the fitted values is equal to 1.8×10^{-6}. The $^3H_4$–$^3P_2$ transition was omitted from the Judd–Ofelt analysis due to the anomalous behaviour of this transition [20]. An inclusion of this transition often leads to a negative value of the Ω_2 intensity parameters, which is unphysical, as well as much larger value of the rms deviation. By means of these three Ω_t intensity parameters the radiative transition probabilities A_J and branching ratios β from the excited $^3P_1$, $^3P_0$ and $^1D_2$ states to lower lying states were calculated. These calculated A_J and β values together with radiative lifetimes τ_{rad} for excited states of Pr^{3+} ions in the lead borate glasses are reported in table 2. The luminescence branching ratios β for $^3P_0$–$^3H_4$ and $^1D_2$–$^3H_4$ transitions are relatively higher than the other ones from both $^3P_0$ and $^1D_2$ levels. Values of the $^3P_0$–$^3H_4$ and $^1D_2$–$^3H_4$ radiative transition probabilities equal to 26 060 and 1357 s^{-1} were compared to the other systems. Basing on literature data, they are situated in the medium range. The A_J value for the $^3P_0$–$^3H_4$ transition is higher than the one (14 271 s^{-1}) obtained for alkali borate glass [21], but smaller than those (34 772 and 40 885 s^{-1}) obtained for lead tellurite and lead titanate glasses [2], respectively. A similar situation is observed for the $^1D_2$–$^3H_4$ transition, where A_J is considerably higher than that obtained for alkali borate glass (753 s^{-1}) and comparable to the PbO–TeO$_2$ (1225 s^{-1}) and PbO–TiO$_2$ (1348 s^{-1}) systems; but it is smaller in comparison to the borate crystals (1872 s^{-1}) in the Ca$_4$GdO(BO$_3$)$_3$ system [22].

The concentration dependent emission spectra of Pr^{3+} ions in lead borate glasses are presented in figure 2. We observe two bands at room temperature in the 15 400–21 000 cm^{-1} spectral ranges, which are different in luminescence intensities. The luminescence spectrum of the sample doped with 0.5 wt% of Pr^{3+} ions consists of a strong intense line associated with the $^1D_2$–$^3H_4$ transition and a considerably weaker band corresponding to the $^3P_0$–$^3H_4$ transition. Both relative band intensities are changed on increasing the Pr concentration. Thus, the luminescence intensity of the $^1D_2$–$^3H_4$ line decreases with the increasing intensity of the $^3P_0$–$^3H_4$ line, when the praseodymium concentration increases from 0.5% to 2.5%. Differences in intensity character are connected with nonradiative processes, which have a considerable share in the $^3P_0$ and $^1D_2$ excited state relaxation. The energy separation between the $^3P_0$ and $^1D_2$ levels is equal to 3800 cm^{-1}, whereas the energy gap between the $^1D_2$ and $^1G_4$ levels is found to be 6800 cm^{-1}. In the PbO–B$_2$O$_3$ system, the maximal phonon energy

Table 2. Calculated radiative transition rates A_J, luminescence branching ratios β and corresponding radiative lifetimes τ_{rad} for Pr^{3+} in lead borate glasses.

Transition	Wavelength λ (nm)	A_J (s^{-1})	τ_{rad} (μs)	β
$^3P_1-^3H_4$	472	9 468	22	0.21
$^3H_5$	530	15 583		0.34
$^3H_6$	611	4 080		0.09
$^3F_2$	626	2 976		0.07
$^3F_3$	686	8 308		0.18
$^3F_4$	705	4 709		0.10
$^1G_4$	898	487		<0.01
$^1D_2$	2331	10		0.01
$^3P_0-^3H_4$	485	26 060	21	0.55
$^3H_6$	632	6 445		0.14
$^3F_2$	648	8 779		0.18
$^3F_4$	734	5 324		0.11
$^1G_4$	944	877		0.02
$^1D_2$	2675	6		<0.01
$^1D_2-^3H_4$	592	1 357	272	0.37
$^3H_5$	686	26		0.01
$^3H_6$	828	443		0.12
$^3F_2$	856	484		0.13
$^3F_3$	973	116		0.03
$^3F_4$	1012	871		0.24
$^1G_4$	1460	378		0.10

of the host ($\hbar\nu = 1300$ cm^{-1}) is associated with the stretching vibrations of the BO_3 groups. Therefore, only three phonons are needed to cover the former energy gap, while multiphonon relaxation is not able to bridge the latter energy gap. From this point of view, the $^1D_2$ level is populated by fast multiphonon non-radiative relaxation from the higher lying $^3P_0$ state. In consequence, emission from both $^3P_0$ and $^1D_2$ levels was detected. For low Pr concentration an intense luminescence from the $^1D_2$ level has been observed. With increasing concentration the radiative $^1D_2$ emission is quenched and weak luminescence corresponding to the $^3P_0-^3H_4$ transition appears to be relatively important.

Figure 3 shows the decay profiles of the $^1D_2$ level of Pr^{3+} ions in the lead borate glasses, measured at room temperature. The luminescence decay of the $^3P_0$ level is very fast, usually below 10 μs, and is difficult to precisely measure as a function of activator concentration. For 0.1 wt% of Pr concentration, the τ value of the $^1D_2$ lifetime is close to 39 μs, and it decreases to 2 μs with increasing (4 wt%) of Pr concentration. Thus, the quantum efficiency η of the $^1D_2$ excited state decreases from 14.3% to 0.7%. Also, changes are observed in the decay character. Luminescence decays are exponential for low activator concentration and become non-exponential and faster for higher Pr concentration. The behaviour results in the presence of luminescence from the $^1D_2$ level when the $^3P_0$ state is excited, and a significant difference between calculated and measured lifetimes for low Pr-doped sample suggests that multiphonon relaxation plays a dominant role. Additionally, the intense luminescence quenching and strong concentration dependence of luminescence band intensity clearly indicate the contribution of non-radiative energy transfer processes to the Pr excited state relaxation in the lead borate glasses. Therefore, activator–activator interactions should be considered in detail.
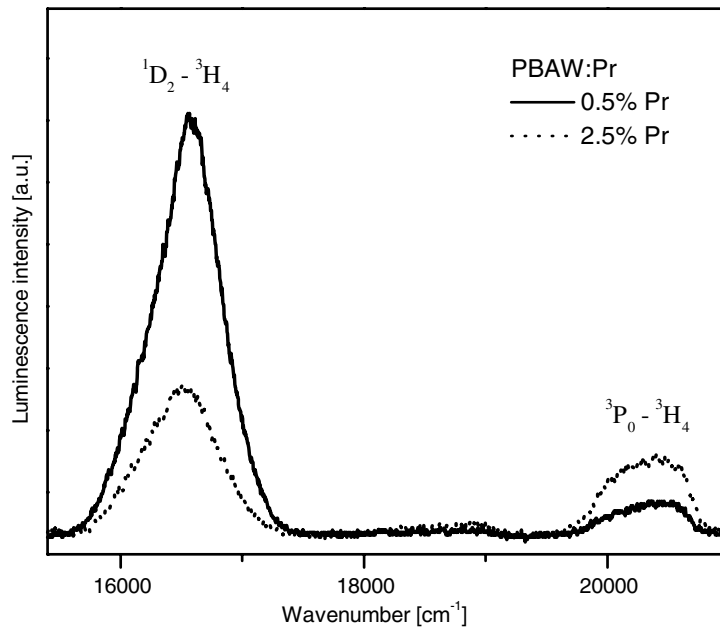
Figure 2. Emission spectra of Pr-doped lead borate glasses.

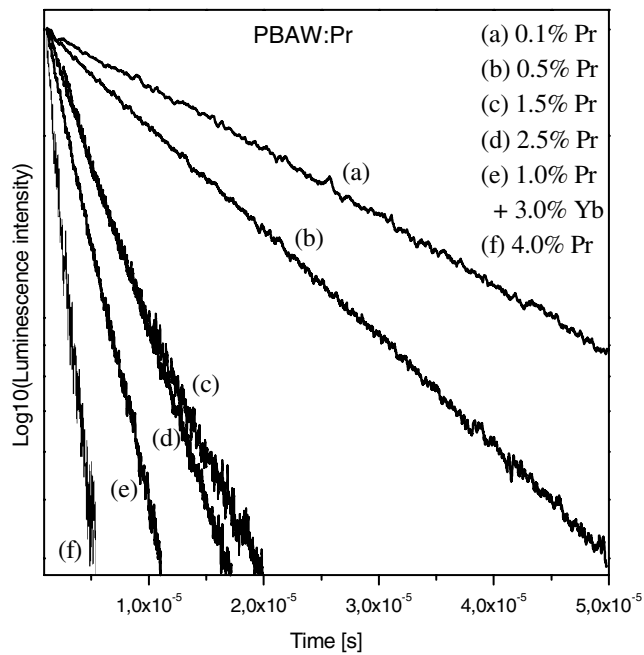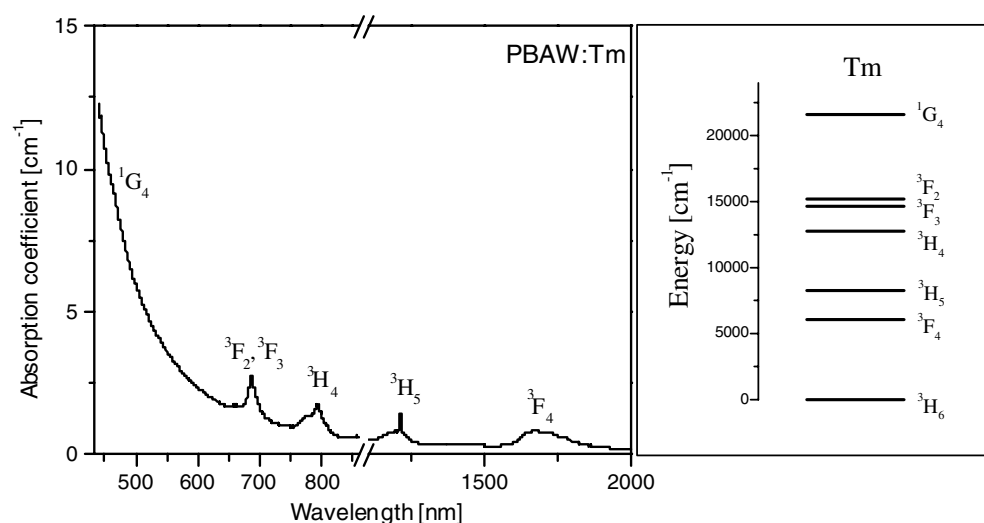

Figure 3. Room temperature $^1D_2$ luminescence decays in Pr-doped lead borate glasses.

4.1.2. Thulium. Figure 4 shows the room temperature absorption spectrum of Tm^{3+}-doped lead borate glass in the range from 435 nm up to 2000 nm. The spectrum consists of several inhomogeneously broadened transitions from the $^3H_6$ ground state to the $^3F_4$, $^3H_5$, $^3H_4$, $^3F_3$, $^3F_2$

Figure 4. Absorption spectrum and energy level scheme of Tm-doped lead borate glass.

Table 3. Measured and calculated oscillator strengths for Tm^{3+} ions in lead borate glasses. Transitions are from the $^3H_6$ ground state to the levels indicated. With $^3H_5$ level: $\Omega_2 = 2.93 \pm 0.42$, $\Omega_4 = 0.58 \pm 0.35$, $\Omega_6 = 1.60 \pm 0.10$ (in 10^{-20} cm^2 units); rms = 6.4×10^{-8}. Without $^3H_5$ level: $\Omega_2 = 2.92 \pm 0.16$, $\Omega_4 = 0.59 \pm 0.14$, $\Omega_6 = 1.55 \pm 0.04$ (in 10^{-20} cm^2 units); rms = 1.8×10^{-8}.

| | | Oscillator strengths | | | | | |
| | | With $^3H_5$ level | | | Without $^3H_5$ level | | |
Levels	Energy ν (cm^{-1})	$P_{meas.}$ ($\times 10^{-6}$)	$P_{calc.}$ ($\times 10^{-6}$)	Residuals ($\times 10^{-6}$)	$P_{meas.}$ ($\times 10^{-6}$)	$P_{calc.}$ ($\times 10^{-6}$)	Residuals ($\times 10^{-6}$)
$^3F_4$	5 800	2.240	2.247	0.007	2.240	2.237	0.003
$^3H_5$	8 400	2.090	1.927	0.163	—	—	—
$^3H_4$	12 650	3.130	3.193	0.063	3.130	3.133	0.003
$^3F_2, ^3F_3$	14 650	4.320	4.442	0.122	4.320	4.319	0.001
$^1G_4$	21 900	0.520	0.657	0.137	0.520	0.656	0.136

and $^1G_4$ excited states belonging to the $4f^{12}$ configuration. The measured P_{meas} and calculated P_{calc} oscillator strengths for all measured absorption transitions are shown in table 3. The rather high value (6.4×10^{-8}) of rms deviation is mainly due to too high discrepancy between the measured and calculated oscillator strengths of the $^3H_6$–$^1G_4$ and $^3H_6$–$^3H_5$ transitions. The first one is located on the tail of the multiphonon absorption edge of the glass and strongly influences the fitting procedure. The second one is connected with contributions of magnetic dipole line strengths. From this point of view, the latter transition can be excluded in the fitting. Finally, an excellent fit was obtained between the experimental and calculated oscillator strengths, as indicated by the rms deviation being equal to 1.8×10^{-8}. Thus, the resulting set of Judd–Ofelt intensity parameters was found to be $\Omega_2 = 2.92 \pm 0.16$, $\Omega_4 = 0.59 \pm 0.14$, $\Omega_6 = 1.55 \pm 0.04$ in 10^{-20} cm^2 units. Then, they were applicable for radiative transition probabilities calculations. The calculated radiative transition probabilities A_J together with luminescence branching ratios β and corresponding radiative lifetimes τ_{rad} for Tm^{3+} ions in lead borate glasses are given in table 4. Values such as radiative transition rates or calculated

Table 4. Calculated radiative transition rates A_J, luminescence branching ratios β and corresponding radiative lifetime τ_{rad} for Tm^{3+} in lead borate glasses.

Transition	Wavelength λ (nm)	A_J (s^{-1})	τ_{rad} (μs)	β
$^1D_2$–$^3H_6$	358	7 319	31	0.23
$^3F_4$	453	19 595		0.61
$^3H_5$	513	206		<0.01
$^3H_4$	656	2 579		0.08
$^3F_3$	730	1 367		0.045
$^3F_2$	781	786		0.045
$^1G_4$	1 667	146		<0.01
$^1G_4$–$^3H_6$	457	1 142	293	0.34
$^3F_4$	621	298		0.09
$^3H_5$	741	1 447		0.42
$^3H_4$	1 081	469		0.14
$^3F_3$	1 299	35		0.01
$^3F_2$	1 471	22		<0.01
$^3F_2$–$^3H_6$	662	1 459	387	0.56
$^3F_4$	1 075	771		0.30
$^3H_5$	1 493	340		0.13
$^3H_4$	4 082	17		0.01
$^3F_3$	11 111	—		—
$^3F_3$–$^3H_6$	704	3 195	276	0.88
$^3F_4$	1 191	118		0.03
$^3H_5$	1 724	291		0.08
$^3H_4$	6 452	25		0.01
$^3H_4$–$^3H_6$	791	1 853	497	0.92
$^3F_4$	1 460	145		0.07
$^3H_5$	2 353	15		0.01
$^3H_5$–$^3H_6$	1 191	404	2457	0.99
$^3F_4$	3 846	3		0.01
$^3F_4$–$^3H_6$	1 724	275	3636	1.00

lifetimes are compared with those obtained for alkali borate glasses and other PbO-based systems. The same trend in order of calculated values for Tm^{3+} ions as for Pr^{3+} ions has been observed. These values are found to be in the medium range, between alkali borate and PbO-based systems. For example, the $^1G_4$ radiative lifetime τ_{rad} is close to 293 μs ($A_T = 3413$ s^{-1}) for Tm^{3+} in lead borate glass (table 3); it is smaller than $\tau_{rad} = 1419$ μs ($A_T = 704$ s^{-1}) and $\tau_{rad} = 880$ μs ($A_T = 1137$ s^{-1}) values obtained for alkali borate glasses [23] and borate crystals in the $Ga_4GdO(BO_3)_3$ system [24], respectively. However, it is higher in comparison to the $\tau_{rad} = 175$ μs ($A_T = 5717$ s^{-1}) value obtained for the PbO–Bi_2O_3–Ga_2O_3 glassy system [25].

Direct excitation of the $^1G_4$ state brings about luminescence, which consists of three spectral lines associated with transitions to the $^3H_6$, $^3F_4$ and $^3H_5$ levels. Two of them, the $^1G_4$–$^3H_5$ and $^1G_4$–$^3F_4$ emission lines in the 12 000–17 000 cm^{-1} spectral range detected at room temperature, are shown in figure 5. Luminescence decays of the $^1G_4$ level were recorded with samples containing 0.5% and 2.5% of thulium (figure 6). For low Tm concentration an exponential decay curve with a time constant of 74 μs was registered. For the 2.5% Tm-doped
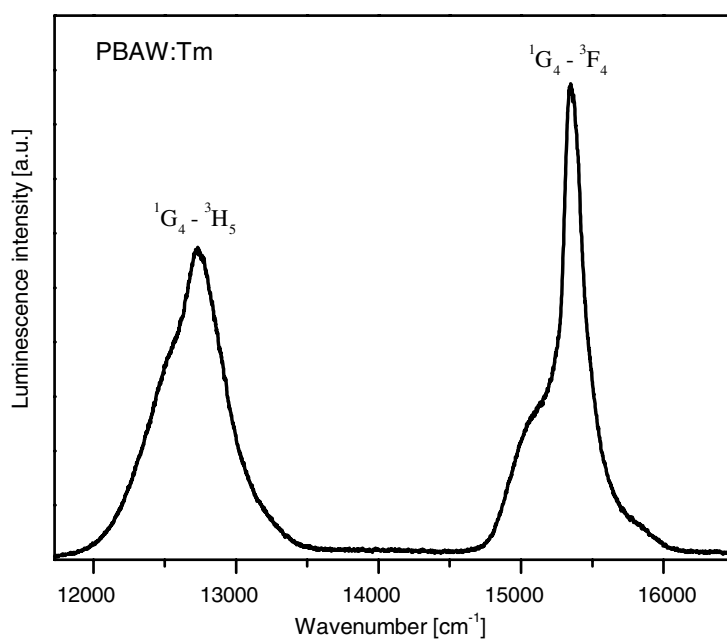
Figure 5. Emission spectrum of Tm-doped lead borate glass.

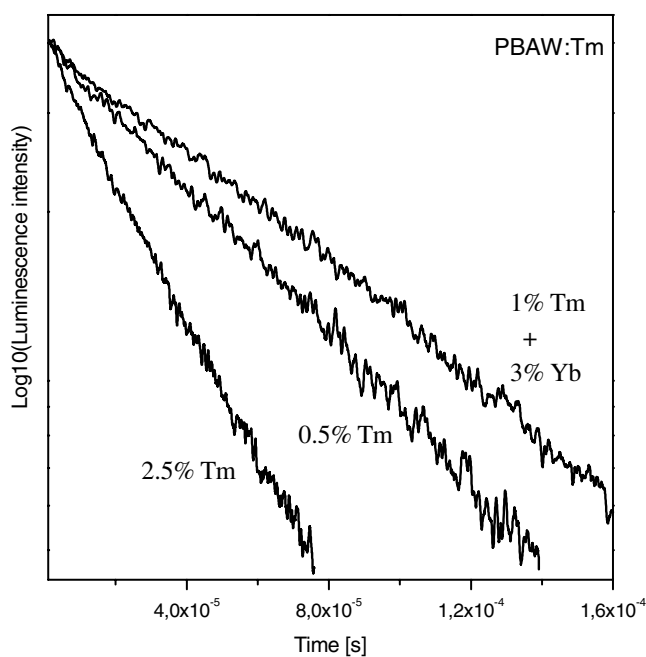**Figure 6.** Room temperature $^1G_4$ luminescence decays in Tm-doped lead borate glasses.

sample, the luminescence decay becomes non-exponential in character and the $^1G_4$ lifetime decreases to 35 μs. Thus, the quantum efficiency η of the $^1G_4$ excited state decreases from 25.3% to 11.9%. In contrast to the praseodymium ions, the second doping of an optically

active ion (Yb) significantly changed the $^1G_4$ luminescence decay curve of Tm^{3+} ions in lead borate glasses. For the doubly doped sample (1% Tm + 3% Yb), the value of the $^1G_4$ lifetime increases from 74 to 101 μs.

For low thulium concentration in lead borate glass the τ and η values are smaller than those obtained for InF_3-based glass ($\tau = 634$ μs, $\eta = 77.8\%$) due to the completely different mechanism of $^1G_4$ excited state relaxation. Owing to the relatively large energy gap ($\sim$5300 cm^{-1}) between the $^1G_4$ level and the next lower lying $^3F_2$ levels, multiphonon emission in the fluoride host characterized by a cut-off frequency of 500 cm^{-1} is not efficient. Therefore mainly radiative transitions from the $^1G_4$ level have been observed in the InF_3-based system [26]. In the PbO–B_2O_3 system, the maximal phonon energy of the host ($\hbar\nu = 1300$ cm^{-1}) is much larger; accordingly only four phonons can easily cover the energy gap. Thus, multiphonon emission significantly contributes to the $^1G_4$ relaxation of Tm^{3+} ions in lead borate glasses. Also, this is a reason for the lack of luminescence from the $^3H_4$ and $^3F_4$ states. For higher Tm concentration the activator–activator interaction appears to be important. Hence, further analysis is needed to clarify whether the concentration quenching is due to cross-relaxation between pairs of Tm^{3+} ions or to energy migration among Tm^{3+} ions to quenching centres.

4.1.3. Pr–Pr and Tm–Tm interactions. A convenient way to explain the mechanism of non-radiative energy transfer processes is luminescence decay curve analysis. With rare earth ion concentration increasing, the measured lifetimes of excited states significantly decrease, which indicates that activator–activator relaxation processes play an important role. Thus, one of the following two mechanisms of energy transfer processes resulting in luminescence quenching can be dominant. The first of them is attributed to the cross-relaxation between pairs of rare earth ions. The second possible process is connected with migration of the excitation energy, which can accelerate the decay by an energy transfer to the structural defects acting as energy sinks. The latter mechanism of energy transfer processes of Pr^{3+} ions has been observed in lithium tetraborate glasses [27]. Independently of praseodymium concentration, the exponential time evolution of the luminescence decays suggests that $^1D_2$ decay is diffusion limited and that there is a considerable migration of excitation energy before cross-relaxation occurs.

In our case, the $^1D_2$ luminescence decays deviate from simple exponential to non-exponential dependence when the praseodymium concentration increases (figure 3). Praseodymium ions play a dual role as donors and acceptors. For low praseodymium concentration, only a small fraction of the total number of excited donors are within the effective interaction sphere of an acceptor, and direct donor–acceptor relaxation contributes less to the overall decay. In consequence, the non-exponential portion of the decays is correspondingly smaller in comparison to the ones observed for samples with higher Pr content. The same situation is observed for the donor–acceptor relaxation from the $^1G_4$ state of thulium ions (figure 6). This indicates that non-radiative processes like cross-relaxation among the donor systems dominate and influence the direct donor–acceptor energy transfer in lead borate glasses. This is similar to what has been observed for Pr^{3+} ions in zinc borate [28] and lead germanate [29] glasses.

From this point of view, the decay curves were fitted by the Inokuti–Hirayama (I–H) model, which can be applicable when donor–acceptor transfer is much faster than migration. Results of the fitting procedure using the I–H model are given in table 5. The I–H model gives a reasonably good fit for all samples with Pr and Tm ions except the 2.5% and 4% Pr-doped samples. The fitting for the highly Pr concentrated samples shows a small deviation along the whole decay. However, a fit with $s = 8, 10$ applied to the decay curves of 2.5% and 4%

Table 5. Results of the fitting of the luminescence decay curves from the $^1D_2$ level of Pr^{3+} and $^1G_4$ level of Tm^{3+} ions obtained using the Inokuti–Hirayama model. The molar ion concentrations, the α values, the critical transfer distances, the donor–acceptor interaction parameters and the energy transfer probabilities are reported.

| Ln^{3+} (wt%)		N_a (10^{20} ion cm^{-3})	α	R_0 (Å)	C_{da} (10^{-51} m^6 s^{-1})	W_{da} (s^{-1})
Pr	0.1	0.190	0.02	5.21	0.513	25 650
	0.5	0.952	0.09	5.03	0.648	40 010
	1 (+3Yb)	1.904	0.17	4.94	2.422	166 653
	1.5	2.856	0.14	4.04	0.483	111 086
	2.5	4.760	0.16	3.58	0.276	133 321
	4.0	7.616	0.26	3.57	1.035	499 955
Tm	0.5	0.810	0.10	5.50	0.374	13 511
	1 (+3Yb)	1.620	0.17	5.21	0.198	9 900
	2.5	4.020	0.40	5.12	0.515	28 588

of Pr^{3+} ions did not evidence any importance of other multipolar processes. In spite of this fact, we cannot unambiguously exclude the possibility of a migration mechanism in highly Pr concentrated lead borate glasses. This also results in unexpectedly smaller values of the critical radius R_0 for highly Pr-doped samples.

The critical transfer distance R_0 is defined as the separation at which the probability of energy transfer between a donor–acceptor pair equals the intrinsic decay rate τ_0^{-1}. The R_0 value is changed from 5.5 to 5 Å, when the Tm concentration increases from 0.5% to 2.5%. Similar values of about 5 Å were obtained for less concentrated samples with Pr^{3+} ions. They are smaller than those (8.2–8.8 Å) obtained for Pr^{3+} ions in zinc borate glasses [28]. The R_0 values and measured lifetimes τ_0 were used to calculate the donor–acceptor interaction parameters and the energy transfer probabilities given by $C_{da} = R_0^6\tau_0^{-1}$ and $W_{da} = C_{da}R_0^{-6}$ relations, respectively. These values are roughly one order of magnitude smaller than those obtained for Tm^{3+} ions in borate crystals [24]. Comparison of W_{da} values indicates higher self-quenching of Pr^{3+} emission than that of Tm^{3+} ions in the lead borate glasses.

4.2. Infrared spectroscopy

Figure 7 shows infrared spectra of lead borate glasses singly doped with Pr^{3+} and Tm^{3+} ions in 4000–1400 cm^{-1} ranges. The IR spectra exhibit the characteristic H_2O (OH stretching vibration) band located near 3445 cm^{-1} (2.9 μm). This is one of the main reasons for the strong luminescence quenching observed in lead borate glasses. The IR cut-off defined as the intersection between the zero base line and the extrapolation of the IR edge is close to about 7.4 μm, and it is comparable to the values obtained for other PbO-based systems [30].

Figure 8 shows IR spectra of the investigated glasses in the range 1400–400 cm^{-1}. In this spectral region the bands are connected with vibrations of the borate network. The IR spectra consist of four characteristic group of bands [31, 32], identified as B–O–B, Pb–O–B bending vibration and borate ring deformation (400–650 cm^{-1}), BO_3 bending (650–700 cm^{-1}) and stretching vibration of tetrahedral BO_4 group (950–1050 cm^{-1}). The fourth main broad IR absorption region existing at about 1200–1400 cm^{-1} reveals two absorption bands due to stretching of trigonal BO_3 (~1210 cm^{-1}) and tetrahedral BO_4 (~1320 cm^{-1}) groups, respectively. In contrast to the borate glasses, the position of these bands is shifted to the lower frequency region, which may reveal the presence of both ionic and covalent Pb–O bonds in the lead borate system. Addition of Al_2O_3 in the lead borate glasses modifies the
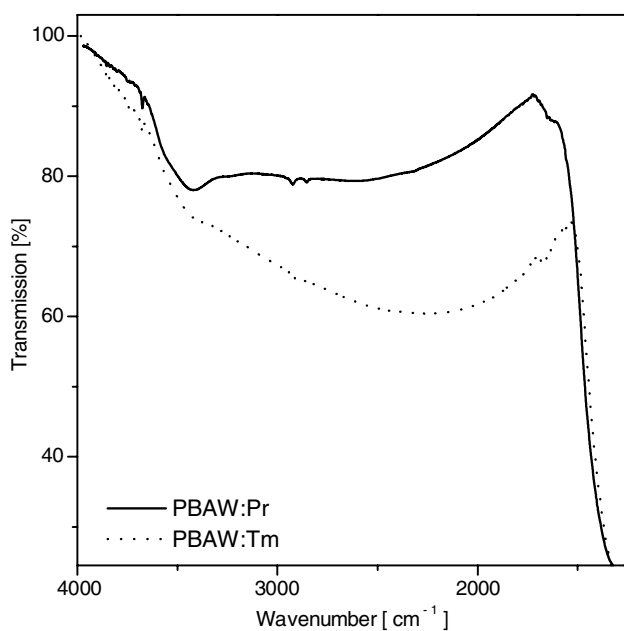
Figure 7. Infrared spectra of lead borate glasses singly doped with Pr^{3+} and Tm^{3+} ions in the 4000–1400 cm^{-1} spectral region.
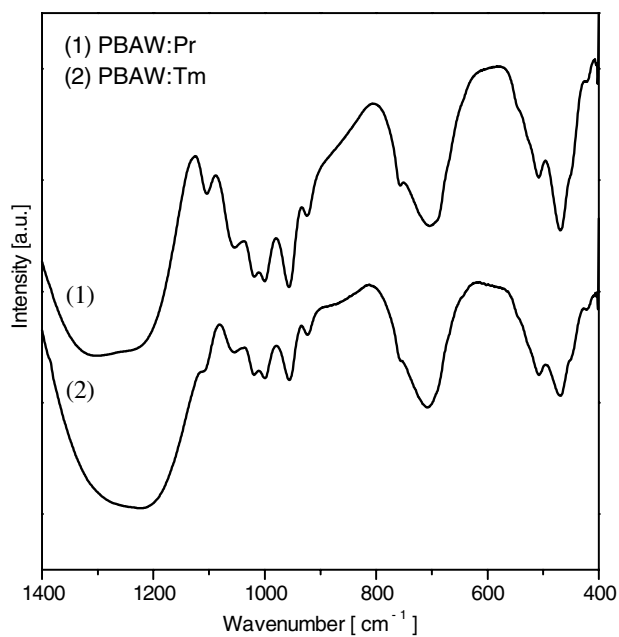
Figure 8. Infrared spectra of lead borate glasses singly doped with Pr^{3+} and Tm^{3+} ions in the 1400–400 cm^{-1} spectral region.

network's structural units, causing a change of boron coordination from BO_3 units to BO_4 units. Additionally, the band at 924 cm^{-1} and the weak shoulder at 835 cm^{-1} correspond to the vibrations of the WO_3 group [33]. The IR spectra clearly show that the intensities of the bands

registered for the 2.5% Tm-doped sample are different in comparison to that one observed for the 2.5% Pr-doped one. In the thulium case, the band centred at 1210 cm^{-1} has higher intensity than the one centred at 1320 cm^{-1}. The same situation causing a change of the intensity ratio is observed for bands located at 700 and 1103 cm^{-1} when compared with the group of bands in the 950–1050 cm^{-1} range. Additionally, the IR spectrum for the 0.5% Tm-doped sample is the same as the one recorded for the 2.5% Pr-doped sample. In the praseodymium case, the infrared spectra are concentration independent. This indicates that the addition of 2.5% of Tm ions to the lead borate glasses partially converts the BO$_4$ into BO$_3$ groups. The structural changes evidenced by the infrared spectroscopy measurements suggest that thulium ions play a role as a modifier in lead borate glasses in contrast to the praseodymium ions. A further analysis of lead borate glasses containing rare earth ions (Pr, Nd, Eu, Er, Tm) indicates that partial BO$_3$ ↔ BO$_4$ conversion as a function of rare earth concentration is observed only for the smaller heavier lanthanides, whereas for the larger lighter lanthanides the concentration effect is independent. However, this problem will be discussed in a separate work.

5. Conclusions

The spectroscopic properties of lead borate glasses singly doped with Pr^{3+} and Tm^{3+} ions have been investigated using optical absorption and emission together with lifetime measurements. The addition of lead oxide to the borate matrix significantly increases the radiative transition rates; however, they are smaller than those obtained for other PbO-based glasses. The results obtained from the concentration dependent emission spectra and luminescence decay curve analysis suggest that multiphonon relaxation and activator–activator interaction play a dominant role in the rare earth excited state relaxation in the lead borate system. The strong luminescence quenching of the ^{1}D$_2$ emission of Pr^{3+} and ^{1}G$_4$ emission of Tm^{3+} ions is connected with cross-relaxation processes and the occurrence of OH$^-$ groups. Additionally, thulium plays a role not only as an optically active ion but it also modifies the borate network in the PbO–B$_2$O$_3$–Al$_2$O$_3$–WO$_3$ glass system, which was observed by infrared spectroscopy.

References

[1] Wachtler M, Speghini A, Gatterer K, Fritzer H P, Ajò D and Bettinelli M 1998 *J. Am. Ceram. Soc.* **81** 2045
[2] Nachimuthu P, Vithal M and Jagannathan R 2000 *J. Am. Ceram. Soc.* **83** 597
[3] Han Y S, Song J H and Heo J 2003 *J. Appl. Phys.* **94** 2817
[4] Choi Y G and Heo J 1997 *J. Non-Cryst. Solids* **217** 199
[5] Song J H, Heo J and Park S H 2003 *J. Appl. Phys.* **93** 9441
[6] Kityk I V, Wasylak J, Benet S, Dorosz D, Kucharski J, Krasowski J and Sahraoui B 2002 *J. Appl. Phys.* **92** 2260
[7] Jayasankar C K and Babu P 1998 *J. Alloys Compounds* **275–277** 369
[8] Ratnakaram Y C, Naidu D T, Kumar A V and Rao J L 2003 *J. Phys. Chem. Solids* **64** 2487
[9] Pan Z, Morgan S H and Long B H 1995 *J. Non-Cryst. Solids* **185** 127
[10] Saisudha M B and Ramakrishna J 1996 *Phys. Rev.* B **53** 6186
[11] Reddy M R, Raju S B and Veeraiah N 2000 *J. Phys. Chem. Solids* **61** 1567
[12] Chen Q, Ferraris M, Menke Y, Milanese D and Monchiero E 2003 *J. Non-Cryst. Solids* **324** 1
[13] Chen Q, Ferraris M, Milanese D, Menke Y, Monchiero E and Perrone G 2003 *J. Non-Cryst. Solids* **324** 12
[14] Cenk S, Demirata B, Öveçoglu M L and Özen G 2001 *Spectrochim. Acta* A **57** 2367
[15] Özen G, Aydinli A, Cenk S and Sennaroğlu A 2003 *J. Lumin.* **101** 293
[16] Judd B R 1962 *Phys. Rev.* **127** 750

[17] Ofelt G S 1962 *J. Chem. Phys.* **37** 511
[18] Carnall W T, Fields P R and Rajnak K 1968 *J. Chem. Phys.* **49** 4412
[19] Inokuti M and Hirayama F 1965 *J. Chem. Phys.* **43** 1978
[20] Peacock R D 1975 *Struct. Bond.* **22** 83
[21] Babu P and Jayasankar C K 2001 *Physica* B **301** 326
[22] Malinowski M, Kowalska M, Piramidowicz R, Łukasiewicz T, Świrkowicz M and Majchrowski A 2001 *J. Alloys Compounds* **323/324** 214
[23] Jayasankar C K and Devi A R 1996 *Opt. Mater.* **6** 185
[24] Dominiak-Dzik G, Ryba-Romanowski W, Gołąb S and Pajączkowska A 2000 *J. Phys.: Condens. Matter* **12** 5495
[25] Heo J, Shin Y B and Jang J N 1995 *Appl. Opt.* **34** 4284
[26] Ryba-Romanowski W, Gołąb S, Dominiak-Dzik G, Żelechower M and Pisarska J 2001 *J. Alloys Compounds* **325** 215
[27] Voda M, Balda R, Al-Saleh W, Sáez de Ocáriz I, Cano M, Lobera G, Macho E and Fernández J 2001 *J. Alloys Compounds* **323/324** 250
[28] Del Longo L, Ferrari M, Zanghellini E, Bettinelli M, Capobianco J A, Montagna M and Rossi F 1998 *J. Non-Cryst. Solids* **231** 178
[29] Balda R, Fernandez J, de Pablos A and Fdez-Navarro J M 1999 *J. Phys.: Condens. Matter* **11** 7411
[30] Lezal D, Pedlikova J, Kostka P, Bludska J, Poulain M and Zavadil J 2001 *J. Non-Cryst. Solids* **284** 288
[31] Ram S and Ram K 1988 *J. Mater. Sci.* **23** 4591
[32] Ganguli M and Rao K J 1999 *J. Solid State Chem.* **145** 65
[33] Ovcharenko N V and Smirnova T V 2001 *J. Non-Cryst. Solids* **291** 121